Korean Journal of Remote Sensing, Vol.25, No.6, 2009, pp.517~529

Fusion Techniques Comparison of GeoEye-1 Imagery

Yonghyun Kim*†, Yongil Kim, and Younsoo Kim***

*Satellite Data application Department, Satellite Information Research Institute, Korea Aerospace Research Institute
**Department of Civil and Environmental Engineering, Seoul National University

Abstract : Many satellite image fusion techniques have been developed in order to produce a high resolution multispectral (MS) image by combining a high resolution panchromatic (PAN) image and a low resolution MS image. Heretofore, most high resolution image fusion techniques have used IKONOS and QuickBird images. Recently, GeoEye-1, offering the highest resolution of any commercial imaging system, was launched. In this study, we have experimented with GeoEye-1 images in order to evaluate which fusion algorithms are suitable for these images. This paper presents compares and evaluates the efficiency of five image fusion techniques, the *à trous* algorithm based additive wavelet transformation (AWT) fusion techniques, the Principal Component analysis (PCA) fusion technique, Gram-Schmidt (GS) spectral sharpening, Pansharp, and the Smoothing Filter based Intensity Modulation (SFIM) fusion technique, for the fusion of a GeoEye-1 image. The results of the experiment show that the AWT fusion techniques maintain more spatial detail of the PAN image and spectral information of the MS image than other image fusion techniques. Also, the Pansharp technique maintains information of the original PAN and MS images as well as the AWT fusion technique.

Key Words : Image fusion, Comparative analysis, GeoEye-1.

1. Introduction

Terms such as merging, combination, synergy, integration, and several others that express more or less the same concept have since appeared in the literature. In the remote sensing community, the following definitions have been adopted but have subtle difference: Pohl and Van Genderen (1998) define image fusion as the combination of two or more different images to form a new image by using a certain algorithm. Wald (1999) defines data fusion as a formal framework in which means and tools are expressed for the alliance of data originating from different sources. According to this definition, fusion aims at obtaining information of greater quality; the exact definition of great quality will depend upon the application. According to Piella (2003), fusion is the combination of pertinent (or salient) information in order to synthesize an image that is more informative and more suitable for visual perception or computer processing, where the pertinence of the information is also dependent on the application task (Thomas *et al*.,

Received December 7, 2009; Accepted December 22, 2009.
† Corresponding Author: Yonghyun Kim (kyh@kari.re.kr)

2008).

Many researchers have addressed the problem of image fusion for remote sensing applications. The most common approaches for fusing a panchromatic (PAN) image with a multispectral (MS) image are based on the intensity-hue-saturation technique (IHS). This technique aims at enhancing the spatial details, but it also produces significant spectral distortion. High pass filtering fusion techniques, which are based on injecting high frequency components into interpolated versions of a MS image, have shown better performance by improving the quality of spatial details, resulting in better visual effects. Other methods considered in the remote sensing literature include approaches based on Principal Component Analysis (PCA) and the wavelet transform (WT). The standard WT fusion techniques replaces the high frequency component of the MS images with that of the PAN image by working in the wavelet domain and then synthesizing the fused image by applying the inverse WT (Joshi *et. al*, 2006). Currently used wavelet based image fusion techniques are mostly based on two computation algorithms: the Mallat algorithm and the *à trous* algorithm. The Mallat algorithm based dyadic WT, which use decimation, is not shift invariant and exhibits artifacts due to aliasing in the fused image. In contrast, the *à trous* algorithm based dyadic WT techniques, which do not use decimation, are shift invariant, a characteristic that makes them particularly suitable for image fusion (Wang *et al*., 2005).

Heretofore, most high resolution image fusion techniques have used the IKONOS (Chu and Zhu, 2008; Dou *et al*., 2007; González-Audácana *et al*., 2006; Kalpoma *et al*., 2007; Tu *et al*., 2004; Tu *et al*., 2007) and the QuickBird (Aiazzi *et al*., 2006; Garzelli and Nencini, 2005; Khan *et al*., 2008; Nikolakopoulos, 2008; Otazu *et al*., 2005) data sets or both (Aan æ s *et al*., 2008; Aiazzi *et al*., 2007; Ling *et al*., 2007; Zhang and Hong, 2005), and many researchers have developed fusion techniques to obtain good fused images. Also, some review (Thomas *et al*., 2008) or comparative analysis (Wang *et al*., 2005; Švab and Oštir, 2006; Nikolakopoulos, 2008) papers have been reported; however, they also used the IKONOS or QuickBird data sets. Recently, GeoEye-1, offering the highest resolution of any commercial imaging system, was launched. In this paper, we have experimented with GeoEye-1 images in order to evaluate which fusion algorithms are

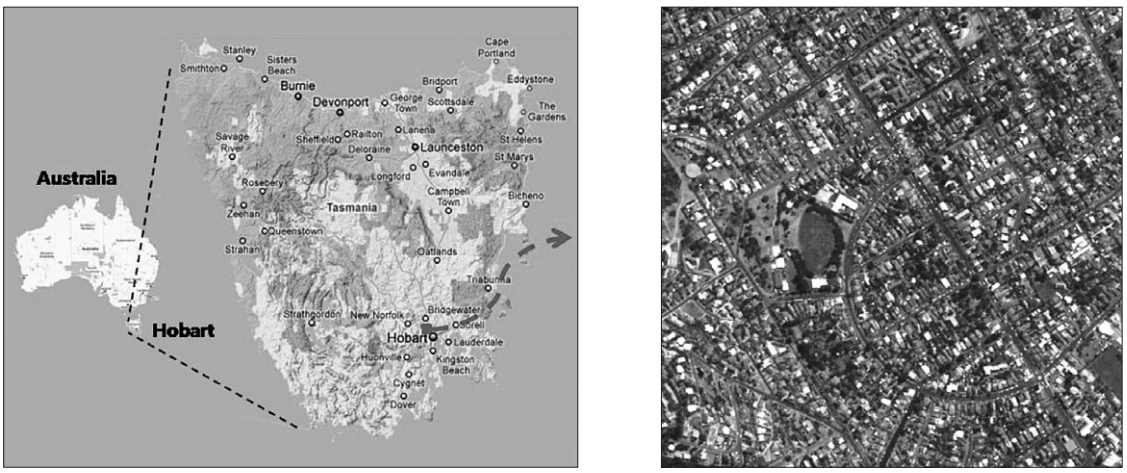

Fig. 1. Study Area in Hobart City, Australia.

suitable for use with these images.

In this paper, five different fusion techniques, the *à trous* algorithm based additive wavelet transformation (AWT) fusion techniques, the PCA fusion technique, Gram-Schmidt (GS) spectral sharpening, Pansharp, and Smoothing Filter based Intensity Modulation (SFIM) fusion techniques, were applied to a GeoEye-1 image in order to assess the quality of the fused images and to determine which fusion algorithms are suitable for GeoEye-1 images. For this experiment, a GeoEye-1 image of Hobart, Australia is used. The spectral quality was compared by using a spatially degraded image and the spatial quality was compared by using an image that is not spatially degraded.

There are five sections in this paper. Section 2 introduces the study area and GeoEye-1 image. Section 3 describes the five image fusion techniques. Section 4 provides the results of the experiment, and section 5 gives our conclusion.

2. The study area in this research

Most color distortion in a fused image appears in areas having much vegetation rather than typical urban areas, because MS band does not fall within the spectral range of the PAN band. For example, in case of the IKONOS sensor, the blue band mostly falls outside the 3-dB cutoff of the PAN band, and hence the blue band is particularly critical (Zhang, 2004). Furthermore, the response of the PAN band is extended beyond the NIR band. Consequently, vegetation appears with relatively high reflectance in the NIR and PAN bands, while having low reflectance in the R-G-B bands (Tu *et al*., 2004). Therefore, it is important to identify which fusion techniques are suitable for vegetation areas. Also, with respecting to the views required for practical applications, urban areas are important, examples being feature detection (Filippidis *et al*., 2000) and land cover classification (Huang and Te-Ming, 2003). Therefore, we used a dataset where some of the area is covered by green vegetation and some of the area is covered by urban features.

The study area of this research is Hobart City, Australia. Hobart is the state capital and the most populous city of the Australian island state of Tasmania. The research area is located in the state's south east region on an estuary of the Derwent River (ranging from 147°8′ 25″E, 42°2′ 40″S to 147°8′ 40″ E, 42°2′ 68″S). The size of the used MS image is 512 × 512 pixels, and the size of the PAN image, captured on February 5, 2009, is 2048 × 2048 pixels. As shown in Fig. 1, the study area is covered by residential areas and green vegetation. GeoEye-1 offers the highest resolution of any commercial imaging system and provides MS and PAN data with spatial resolution of 1.65 and 0.41 m, respectively. However, we experimented on PAN data with a spatial resolution of 0.50m, because of the terms of GeoEye's license with the U.S. government. The MS image has four wavelength bands: blue [450-510 nm], green [510-580 nm], red [655-690 nm], and near infrared [780-920 nm] and the wavelength of the PAN image is 450-800 nm. The GeoEye-1 data was collected at 11bits per pixel. This means that there is more definition in the gray scale values and the viewer can see greater detail in the image. In order to benefit from this additional information, the processing and evaluation were entirely based on the original 11 bits data, and the data was converted to 8 bits for display purposes only (Wang *et al*., 2005).

3. Image fusion techniques

Since the launch of SPOT-1 (providing high resolution (10m) PAN images and low resolution

(20m) MS images) in 1986, many fusion techniques have been presented. Some are very simple, based on algebra functions, and others are quite sophisticated based on wavelet theory (Nikolakopoulos, 2008). We have experimented five fusion techniques, AWT, PCA, GS spectral sharpening, Pansharp, and the SFIM for the fusion of GeoEye-1 image. The Mallat algorithm based wavelet fusion techniques were excluded because of artifacts in fused images (González-Audácana *et al*.,2004; Hill *et al*., 2002), the IHS fusion technique was also excluded because it is limited to three bands at a time and severely distorts the spectral information of MS image.

1) *à trous* algorithm based wavelet fusion technique

A discrete approach to the wavelet transform can be done with several different algorithms. However, not all algorithms are well suited for all the problems. The popular Mallat's algorithm (Mallat, 1989) uses an orthonormal basis, but the transform is not shift invariant, which can be a problem in signal analysis, pattern recognition or, as in our case, data fusion (Núñez *et al*., 1999). The term "*à trous*" was originally introduced by Dutilleux. (1989). It is based on the undecimated dyadic wavelet transform and is particularly suitable for signal processing since it is isotropic and shift invariant and does not create artifacts when used in image processing (Shensa, 1992, Murtagh and Starck, 2000). Given an image p, the sequence of its approximations by multiresolution decomposition is $F_1(p) = p_1$, $F_2(p1) = p_2$, ... The wavelet planes ω_j of Eq. (1) are computed as the differences between two consecutive approximations where n refers to the decomposition level. To construct the sequence, this algorithm performs successive convolutions with a filter obtained from an auxiliary function named scaling function. The use of a B3 cubic spline yields a dyadic low pass scaling function such as $h_0 = (1/16)[1,4,6,4,1]$ in one dimension. Also, we can write the reconstruction formula as Eq. (2).

$$\omega_j = p_{j-1} - p_j, j=1, \cdots, n, p_0 = p \quad (1)$$

$$p = p_r + \sum_{j=1}^{n} \omega_j \quad (2)$$

In this representation, the images p_j (j=0,...,n) are version of the original image p at increasing scales (decreasing resolution levels), and p_r is a residual image. The original image p_0 has double resolution than p_1, the image p_1 double resolution than p_2, and so on (Núñez *et al*., 1999). There are several possible ways of using the *à trous* algorithm in image fusion (Wang *et al*., 2005). We follow the ATW fusion technique. The most generally method is to add the wavelet planes of the high resolution image directly to the MS image. The AWT technique can be written as follows, and the PAN image is histogram matched to the MS image:

$$MS_{High} = \sum_{j=1}^{n} \omega_j + MS_{Low} \quad (3)$$

where MS_{High} is fused MS image and MS_{Low} is the low resolution MS image.

2) PCA

In general, the first principal component (PC^1) collects the information that is common to all the bands used as input data in the PCA, i.e., the spatial information, while spectral information that is specific to each band is picked up in the other principal components (Chavez and Kwarteng, 1989). This makes PCA a very adequate technique when merging MS and PAN images. In this case, all the bands of the original MS image constitute the input data. As a result of this transformation, we obtain non correlated new bands, the principal components. The PC^1 is substituted by the PAN image, whose histogram has previously been matched with that of the PC^1. Finally, the inverse transformation is applied

to the whole dataset formed by the modified PAN image and the PC^2 ... PC^n, obtaining in that way a new fused image with the spatial detail of the PAN image incorporated into it (González-Audácana *et al*.,2004). The PCA fusion technique works best when merging images where there is significant overlap of the wavelengths.

3) GS spectral sharpening

In the GS spectral sharpening, which is implemented in the Environment for Visualizing Images (ENVI) program, as described by its inventors (Laben and Brower, 2000), the spatial resolution of the MS image is enhanced by merging the high resolution PAN image with the low spatial resolution MS bands. The main steps of this method are the following. First, a low spatial resolution PAN image is simulated at the same scale of PAN, and the GS transformation is performed on the simulated lower spatial resolution PAN image together with the plurality of lower spatial resolution spectral band images resampled at the same scale of PAN. The simulated lower spatial resolution PAN image is employed as the first band in the GS transformation. After that, the statistics of the higher spatial resolution PAN image are adjusted to match the statistics of the first transform band that result from the GS transformation to produce a modified higher spatial resolution PAN image, and the modified higher spatial resolution PAN image is substituted for the first transform band that results from the GS transformation to produce a new set of transform bands. Finally, the inverse GS transformation is performed on the new set of transform bands to produce the enhanced spatial resolution MS image (Aiazzi *et al*., 2007).

4) Pansharp

A new statistics based fusion called Pansharp was presented by Zhang (2002) and is currently being implemented in the PCI Geomatica software as special module. This statistics based fusion technique solves the two major problems in image fusion: color distortion and operator (or dataset) dependency. It is different from existing image fusion techniques in two principle ways: (1) it utilizes the least squares technique to find the best fit between the grey values of the image bands being fused and to adjust the contribution of individual bands to the fusion result to reduce the color distortion, and (2) it employs a set of statistical approaches to estimate the grey value relationship between all the input bands to eliminate the problem of dataset dependency (i.e., reduce the influence of dataset variation) and to automate the fusion process (Nikolakopoulos, 2008).

5) SFIM

This SFIM (Liu, 2000) technique is based upon a solar radiation and land surface reflection model. The basic idea consists of using the ratio between the high resolution PAN image and its low resolution version, which is obtained by low pass filtering. Spatial details can be injected into the upscaled, coregistered, low resolution MS image without changing its spectral content as:

$$DN(\lambda)_{SFIM} = \frac{DN(\lambda)_{low} DN(\gamma)_{high}}{DN(\gamma)_{mean}} \qquad (4)$$

where DN stands for the digital number, and $DN(\gamma)_{high}$, $DN(\gamma)_{mean}$, $DN(\lambda)_{low}$, and $DN(\lambda)_{SFIM}$ are the values of a pixel in the high spatial resolution PAN, low spatial resolution PAN (obtained after the application of a smoothing low pass filter), upscaled low spatial resolution MS, and the desired high spatial resolution MS images, respectively. The size of the smoothing filter for obtaining the $DN(\gamma)_{mean}$ image is equal to the ratio of the PAN and MS image size. For GeoEye-1, the ratio is equal to 4. Hence, the

used low pass filter is a standard 4 × 4 averaging filter (Khan *et al*., 2008).

4. Experimental Results

This section is divided into three subsections. In Section 4.1, we present a visual comparison of five fused images. Section 4.2 presents a brief overview of the index chosen to assess the spectral and spatial quality of fused images, and Section 4.3 presents a quality comparison of the merged images.

1) Visual Comparison

A visual comparison of the R-G-B band combinations of the fused images was used for the qualitative assessment, since it is a simple, but effective method for showing the major advantages and disadvantages of a fusion technique. R-G-B composites are presented for the original MS image and all the merged images in order to validate the visual evaluation. The fused images of degraded scale were used for comparison with the original MS image and to validate the visual evaluation, more detailed, full scale subset images were used.

The fused image with the AWT technique (see Fig. 3) has similar color with the original MS image, reflecting that the spectral information of the original MS image was preserved. However, with respect to the color of the fused image with the PCA technique (see Fig. 4), the overall scene was slightly brighter. The fused image with GS spectral sharpening (see Fig. 5) was distorted; in particular, the roads and building roofs were highly reflective. In Figs. 6 and 7, the fused images of the Pansharp and SFIM techniques are presented. The color of the Pansharp image shows similar results with the original MS image, indicating that Pansharp preserved the spectral information of the original MS image. On the contrary, SFIM distorted the spectral information of the original MS image, and it did not preserve the spatial texture information of the PAN image.

In the comparison of spatially not degraded scale, the AWT (see Fig. 8) and the Pansharp (see Fig. 11) appeared to be suitable for the fusion of the GeoEye-1 image. The five fusion techniques show subtle differences in roads and roofs. In particular, the PCA (see Fig. 9) and the GS (see Fig. 10) techniques show high reflectance. However, in the case of vegetation areas, the differences are distinct. The PCA and the GS techniques show lower reflectance than the AWT and Pansharp techniques. In the case of the SFIM (see Fig. 12) fusion technique, it was confirmed that the technique was not as effective in preserving spatial detail of the PAN image relative to the other fusion techniques.

2) Quality index

Two kinds of evaluation models are employed to assess the preservation of the information of the MS image and PAN image. First, in order to assess the spectral quality of the fused image, fused image should be compared with the image that the GeoEye-1 sensor would theoretically collect in MS mode if it had a spatial resolution of a PAN image. However, this image does not exist. Therefore, we experimented with a spatially degraded image. Hence, before the fusion process, the GeoEye-1 images were degraded to a factor of 0.25. Consequently, the spectral quality of the merged image was evaluated by comparing the resulting fused image with the original MS image. Second, in order to assess the spatial quality of the merged image, we experimented with the spatially not degraded image and compared it with the original PAN image.

Fig. 2. Original MS image.

Fig. 3. Degrade scale fused image with AWT.

Fig. 4. Degrade scale fused image with PCA.

Fig. 5. Degrade scale fused image with GS.

Fig. 6. Degrade scale fused image with Pansharp.

Fig. 7. Degrade scale fused image with SFIM.

Fig. 8. Full scale subset image with AWT.

Fig. 9. Full scale subset image with PCA.

Fig. 10. Full scale subset image with GS.

Fig. 11. Full scale subset image with Pansharp.

Fig. 12. Full scale subset image with SFIM.

(1) Spectral quality assessment

A good fusion technique has to maintain the spectral information of original MS image when increasing its spatial detail. To measure the spectral distortion due to the fusion process, each fused image was compared to the original MS image, using the Correlation Coefficient (CC) between each band of the original MS image and fused image. It should be as close to 1 as possible. These parameters only allow evaluating the difference in spectral information between corresponding bands of the merged image and the original image. In order to estimate the global spectral quality of the merged images, the *erreur relative globale adimensionnelle de synthèse* index (ERGAS), whose English translation is *relative dimensionless global error* in fusion (Ranchin and Wald, 2000) parameter is used:

$$\mathrm{ERGAS} = 100\frac{d_h}{d_l}\sqrt{\frac{1}{L}\sum_{l=1}^{L}\left(\frac{\mathrm{RMSE}(l)}{\mu(l)}\right)^2} \qquad (5)$$

where d_h is the resolution of the PAN image, d_l is the resolution of MS image, L is the number of spectral band (l) involved in the fusion, $\mu(l)$ is the mean radiance of each spectral band, and Root Mean Square Error (RMSE) is computed between each band of the original MS and the merged image. The lower ERGAS value, the higher the spectral quality of the fused images. Recently, Alparone *et al* (2004) proposed an index, based upon quaternions, for comprehensively assessing the quality of fusion process. The proposed index is called Q4 as it can be used for the global analysis of all four MS bands. The index lies within the interval [0, 1], with 1 being the ideal value. The index is defined as:

$$Q4 = \frac{|\sigma_{Z_A Z_B}|}{\sigma_{Z_A}\cdot\sigma_{Z_B}} \cdot \frac{2\sigma_{Z_A}\cdot\sigma_{Z_B}}{\sigma_{Z_A}^2+\sigma_{Z_B}^2} \cdot \frac{2|\overline{Z_A}|\cdot|\overline{Z_B}|}{|\overline{Z_A}|^2+|\overline{Z_B}|^2} \qquad (6)$$

where $Z_A = a_A + ib_A + jc_A + kd_A$ and $Z_B = a_B + ib_B + jc_B + kd_B$ denote the 4 band reference MS image and the fusion product, respectively, both expressed as quaternions or hypercomplex numbers. This index consists of three parts. The first part is sensitive to the loss of correlation and spectral distortions. The second term measures contrast changes while the last term measures the mean bias of all bands (Tania Stathaki *et al*., 2008). The values of these parameters resulting from the comparison of the fused image are presented in Table 1.

Table. 1. Quantitative assessment of the fusion results

Index		AW	PCA	GS	Pansharp	SFIM	Ideal
CC	B	0.9542	0.9480	0.9485	0.9604	0.9384	
	G	0.9615	0.9574	0.9584	0.9698	0.9436	
	R	0.9621	0.9548	0.9556	0.9695	0.9423	
	NIR	0.8832	0.8937	0.8928	0.8958	0.8931	
	$\overline{CC}$	0.9402	0.9385	0.9388	**0.9489**	0.9294	
SCC	B	0.9951	0.9939	0.9839	0.9833	0.9603	1
	G	0.9956	0.9969	0.9949	0.9930	0.9503	
	R	0.9956	0.9968	0.9933	0.9943	0.9484	
	NIR	0.9923	0.9852	0.9624	0.9756	0.9083	
	$\overline{SCC}$	**0.9946**	0.9932	0.9836	0.9866	0.9418	
Q4		**0.9252**	0.8774	0.8779	0.8870	0.8870	
ERGAS		**3.7559**	4.3462	4.3423	4.1807	4.0796	0

(2) Spatial quality assessment

A good fusion technique must allow the injection, into each band of the MS image, of the spatial detail the MS image would observe if it worked at a spatial resolution similar to that of the PAN image. In order to estimate the spatial quality of the fused image, we follow the procedure proposed by Zhou (1998). First, the spatial detail information present in the two images to be compared is extracted using a Laplacian filter. Second, the correlation between these two filtered images is calculated. A high spatial correlation coefficient (SCC) indicates that much of the spatial detail information of one of the images is present in the other one. The Laplacian filter used to extract the spatial detail of the different image is:

$$\begin{vmatrix} -1 & -1 & -1 \\ -1 & 8 & -1 \\ -1 & -1 & -1 \end{vmatrix} \quad (7)$$

In Table 1, we show the SCC values obtained from fused images and original PAN image.

(3) Experimental results

For the quantitative analysis, the indices CC, SCC, Q4, and ERGAS were calculated. In the assessment of preservation of the spectral information of the MS image, with the AWT technique the best results are obtained in the Q4 and ERGAS index. This means that the AWT technique preserved the global spectral information of the original MS image. The PCA and GS spectral sharpening techniques have similar index values in spatial and spectral assessment. The Pansharp technique provided the highest CC value, and all bands showed the highest CC values. This means that the Pansharp technique is effective in preserving the spectral information of the MS image. The SFIM technique yielded the lowest CC and SCC values, and its ERGAS and Q4 index values were lower than those of the other techniques. Therefore, this technique offered no advantage in fusing the GeoEye-1 image.

5. Conclusion

Demand for more accurate earth observation data has increased. In order to meet this need, or, in other words, to improve the spatial quality without producing color distortion, image fusion techniques are required. In this paper, we compared and evaluated five image fusion techniques and tested a GeoEye-1 image, which provides the highest spatial resolution among commercial satellite images. To investigate the quality of fused images, we used four indexes, namely, CC, SCC, Q4, and ERGAS. The experimental results show that the AWT technique provides a satisfactory result for GeoEye-1 image fusion, delivering the highest Q4 (0.9252) and the lowest ERGAS (3.7559) values. In the case of spatial quality, the AWT technique yielded the highest SCC (0.9946) value among the evaluated fusion techniques. In the visual comparison, it is observed that the fused image provided by the AWT technique is almost equal in quality to the MS image. In the case of commercial software tools, the Pansharp technique yields better results, including the highest value for CC (0.9489) value, than the GS (0.9388) spectral sharpening technique. Also, the Pansharp technique delivered suitable results in SCC (0.9866), and showed similar color with the original MS image. The PCA technique delivered the highest ERGAS (4.3462) values and the SFIM technique yielded unsatisfactory results for GeoEye-1 image fusion, presenting the lowest CC (0.9294) and SCC (0.9418) value.

Acknowledgments

The authors would like to thank HYUNDAI WIA (http://www.hyundai-wia.com/) and GeoEye (http://www.geoeye.com/) for kindly supplying the GeoEye-1 image for this research.

References

Aanæs, H., J.R. Sveinsson, A.A. Nielsen, 2008. Model-based satellite image fusion, *IEEE Transactions on Geoscience and Remote Sensing*, 46(5): 1336-1346.

Aiazzi, B., L. Alparone, S. Baronti, A. Garzelli, M. Selva, 2006. MTF-tailored multiscale fusion of high-resolution ms and pan imagery,

Photogrammetric Engineering and Remote Sensing, 72(5): 591-596.

Aiazzi, B., S. Baronti, M. Selva, 2007. Improving component substitution pansharpening through multivariate regression of ms+pan data, *IEEE Transactions on Geoscience and Remote Sensing*, 45(10): 3230-3239.

Alparone, L., S. Baronti, A. Garzelli, F. Nencini, 2004. A global quality measurement of pan-sharpened multispectral imagery, *IEEE Transactions on Geoscience and Remote Sensing Letters*, 1(4): 313-317.

Chavex P. S. and A. Y. Kwarteng, 1989. Extracting spectral contrast in Landsat Thematic Mapper image data using selective principal component analysis, *Photogrammetric Engineering and Remote Sensing*, 55(3): 339-348.

Chu, H. and W. Zhu, 2008. Fusion of IKONOS satellite imagery using IHS transform and local variation, *IEEE Transactions on Geoscience and Remote Sensing Letters*, 5(4): 653-657.

Dou, W., Y. Chen, X. Li, D.Z. Sui, 2007. A general framework for component substitution image fusion: An implementation using the fast image fusion method, *Computer & Geosciences*, 33(2): 219-228.

Dutilleux, P. 1989. An implementation of the algorithms *à trous* to compute the wavelet transform, in wavelets: time-frequency methods and phase space. J. M. Cobbes, A. Grossman. and Ph. Tchamitchian, Eds. Berlin, Germany: Springer-Verlag, 298-304.

Filippidis, A., L. C. Jain, and N. Martin, 2000, Multisensor data fusion for surface land-mine detection, IEEE Transactions on Systems, Man, and Cybernetics, *Part C: Applications and Reviews*, 30(1): 145-150.

Garzelli, A. and F. Nencini, 2005. Interband structure modeling for pan-sharpening of very high-resolution multispectral images, *Information Fusion*, 6: 213-224.

González-Audácana, M., J.L. Saleta, R. G. Catalán, R. García, 2004, Fusion of multispectral and panchromatic images using improvement IHS and PCA mergers based on wavelet decomposition, *IEEE Transactions on Geoscience and Remote Sensing*, 42(6): 1291-1299.

González-Audácana, M., X. Otazu, O. Fors, J. Alvarez-Mozos, 2006. A low computational-cost method to fuse IKONOS images using the spectral response function of its sensors, *IEEE Transactions on Geoscience and Remote Sensing*, 44(6): 1683-1691.

Hill, P., N. Canagarajah, D. Bull, Image fusion using complex wavelets, Proceeding of 13th British Machine Vision Conference, 2002. 487-496.

Huang, P. S. and T. Te-Ming, A target fusion based approach for classifying high spatial resolution imagery, Proceeding of Workshops Advances Techniques for Analysis of Remotely Sensed Data, 2003. 175-181.

Joshi, M. V. and L. Brunzzone, 2006. A model-based approach to multi-resolution fusion in remotely sensed images, *IEEE Transactions on Geoscience and Remote Sensing*, 44(9): 2549-2562.

Kalpoma, K. and J. Kudoh, 2007. Image fusion processing for IKONOS 1m color imagery, *IEEE Transactions on Geoscience and Remote Sensing*, 45(10): 3075-3086.

Khan, M. M., J. Chanussot, L. Condat, A. Montanvert, 2008. Indusion: fusion of multispectral and panchromatic images using the induction scaling technique. *IEEE Transactions on Geoscience and Remote*

Sensing Letters, 5(1): 98-102.

Laben, C. A. and B.V. Brower, Process for enhancing the spatial resolution of multispectral imagery using pan-sharpening. U.S. Patent 6011875, Jan. 4, 2000. Tech. Rep., Eastman Kodak Company.

Ling, Y., M. Ehlers, E. L. Usery, and M. Madden, 2007. FFT-enhaced IHS transform method for fusing high-resolution satellite images. *ISPRS Journal of Photogrammetry and Remote Sensing*, 61: 381-392.

Liu, J. G., 2000. Smoothing filter-based intensity modulation: A spectral preserve image fusion technique for improving spatial details, *International Journal of Remote Sensing*, 21(18): 3461-3472.

Mallat, S., 1989. A theory for multiresolution signal decomposition: the wavelet representation. *IEEE Transactions on Pattern Analysis and Machine Intelligence*, 11(7): 674-693.

Murtagh, F. and J.L. Starck, 2000. Image processing through multiscale analysis and measurement noise modeling, *Statistics and Computing*, 10(2): 95-103.

Nikolakopoulos, K. G., 2008. Comparison of nine fusion techniques for very high resolution data, *Photogrammetric Engineering and Remote Sensing*, 74(5): 647-659.

Núñez, J., X. Otzau, O. Fors, A. Prades, V. Palà, R. Arbiol, 1999. Multiresolution-based image fusion with additive wavelet decomposition, *IEEE Transactions on Geoscience and Remote Sensing*, 37(3): 1204-1211.

Otazu, X., González-Audácana, M., O. Fors, J. Núñez, 2005. Introduction of sensor spectral response into image fusion methods, Application to wavelet-based methods, *IEEE Transactions on Geoscience and Remote Sensing*, 43(10): 2376-2385.

Piella, G., 2003. A general framework for multiresolution image fusion: from pixels to regions, *Information Fusion*, 4: 259-280.

Pohl, C. and J. L. Van Genderen, 1998. Multisensor image fusion in remote sensing: Concepts, methods and applications, *International Journal of Remote Sensing*, 19(5): 823-854.

Ranchin, T. and L. Wald, 2000. Fusion of high spatial and spectral resolution images: The ARSIS concept and its implementation, *Photogrammetric Engineering and Remote Sensing*, 66(1): 49-61.

Shensa, M. J., 1992. The discrete wavelet transform: wedding the *à trous* and Mallat algorithm, *IEEE Transactions on Signal Processing*, 40(10): 2464-2482.

Švab, A. and K. Oštir, 2006. High-resolution image fusion: methods to preserve spectral and spatial resolution, *Photogrammetric Engineering and Remote Sensing*, 72(5): 565-572.

Tania, S., 2008. Image fusion, Academic Press in an imprint of Elsevier, p. 51.

Thomas, C., T. Ranchin, L. Wald, and J. Chanussot, 2008. Synthesis of multispectral images to high spatial resolution: A critical review of fusion methods based on remote sensing physics, *IEEE Transactions on Geoscience and Remote Sensing*, 46(5): 1301-1312.

Tu, T. M., W. C. Cheng, C. P. Chang, P. S. Huang, and J. C. Chang, 2007. Best tradeoff for high-resolution image fusion to preserve spatial details and minimize color distortion, *IEEE Transactions on Geoscience and Remote Sensing Letters*, 4(2): 302-306.

Tu, T. M., P. S. Huang, C. L. Hung, and C. P. Chang, 2004. A fast intensity-hue-saturation fusion technique with spectral adjustment for IKONOS imagery, *IEEE Transactions on Geoscience and Remote Sensing Letters*, 1(4).

309-312.

Wald, L., 1999. Some terms of reference in data fusion, *IEEE Transactions on Geoscience and Remote Sensing*, 37(3): 1190-1193.

Wang, A., D. Ziou, C. Armenakis, D. Li, and Q. Li, 2005. A comparative analysis of image fusion methods, *IEEE Transactions on Geoscience and Remote Sensing*, 43(6): 1391-1402.

Zhang, Y., A new automatic approach for effectively fusing Landsat 7 as well as Ikonos images, Proceedings of IEEE/IGARSS'02, Toronto, Canada, 4; 2429-2431.

Zhang, Y., 2004. Understanding image fusion, *Photogrammetric Engineering and Remote Sensing*, 70(6): 657-661.

Zhang, Y. and G. Hong, 2005. An IHS and wavelet integrated approach to improve pan-sharpening visual quality of natural colour IKONOS and QuickBird images, *Information Fusion*, 6: 225-234.

Zhou, J., D. L. Civco, and J. A. Silander, 1998. A wavelet transform method to merge Landsat TM and SPOT panchromatic data, *International Journal of Remote Sensing*, 19(4): 743-757.